AGU PUBLICATIONS

Water Resources Research

TECHNICAL REPORTS: METHODS

10.1002/2017WR021629

Key Points:
- Characteristic lengths govern processes related to flow in unsaturated porous media
- These lengths are inferred from data fitted to constitutive laws
- Impact of model selection and parametric uncertainty on lengths' identification is analyzed

Correspondence to:
D. Tartakovsky,
tartakovsky@stanford.edu

Citation:
Assouline, S., Ciriello, V., & Tartakovsky, D. M. (2017). Estimation of intrinsic length scales of flow in unsaturated porous media. *Water Resources Research*, *53*, 9980–9987. https://doi.org/10.1002/2017WR021629

Received 29 JUL 2017
Accepted 21 OCT 2017
Accepted article online 26 OCT 2017
Published online 22 NOV 2017

Estimation of Intrinsic Length Scales of Flow in Unsaturated Porous Media

Shmuel Assouline[1], Valentina Ciriello[2], and Daniel M. Tartakovsky[3]

[1]Department of Environmental Physics and Irrigation, Institute of Soil, Water and Environmental Sciences, A.R.O., the Volcani Center, Rishon LeZion, Israel, [2]Department of Civil, Chemical, Environmental, and Materials Engineering, University of Bologna, Bologna, Italy, [3]Department of Energy Resources Engineering, Stanford University, Stanford, CA, USA

Abstract Characteristic lengths govern processes related to flow in unsaturated porous media, e.g., during drainage or evaporation. One can estimate these lengths, i.e., air-entry pressure head and critical capillary head, from either a water retention curve (WRC) or a hydraulic conductivity function (HCF). We provide new analytical expressions for the characteristic lengths based on a linearized analysis of the WRC and HCF curves. These are then used to investigate the impact of model selection on length-scale estimates, to assess their sensitivity to model parameters, and to provide guidelines for the choice of the alternative expressions under flow scenarios of interest.

1. Introduction

Flow in partially saturated porous media has a number of intrinsic length scales (Miller & Miller, 1956; Roth, 2008; Sposito & Jury, 1985; Tillotson & Nielsen, 1984), which govern phenomena such as dynamics of soil evaporation and drainage (Assouline & Or, 2014; Hoogland et al., 2016; Lehmann et al., 2008; Or et al., 2013). Some of these length scales have been used to delineate the range of applicability of the Richards equation (Or et al., 2015). Definition of such length scales relies on two concurrent conditions: (i) the existence of a capillary gradient that drives the flow, and (ii) the presence of continuous capillary pathways. These conditions are fulfilled only within the range of drainable soil pores, between the air-entry head ψ_{ae} and the critical capillary head ψ_{ch}. The latter is defined as a characteristic length of a porous medium corresponding to the disruption of hydraulic water continuity. Attainment of ψ_{ch} determines the cessation of internal drainage as identified by a concept of field capacity (Assouline & Or, 2014); the corresponding saturation degree S_{ch} can be estimated by means of an appropriate model for the soil water retention curve (WRC). Distance $L_c=|\psi_{ch}|-|\psi_{ae}|$ can then be used to predict transition from capillary-supplied (stage I) evaporation to vapor diffusion-controlled (stage II) evaporation (Lehmann et al., 2008).

Values of ψ_{ch} and L_c can be estimated from an inflection point, $(S^\star, |\psi^\star|)$, of the WRC (see Figure 1a) (Assouline & Or, 2014; Lehmann et al., 2008). For the van Genuchten WRC (hereinafter WRC-vG), this approach yields (Assouline & Or, 2014)

$$|\psi_{ch}|=\frac{1}{\alpha}\left(\frac{n-1}{n}\right)^{\frac{1-2n}{n}}, \qquad L_c=|\psi_{ch}|-|\psi_{ae}|=\frac{1}{\alpha(n-1)}\left(\frac{n}{2n-1}\right)^{\frac{1-2n}{n}}\left(\frac{n-1}{n}\right)^{\frac{1-n}{n}}, \tag{1a}$$

and

$$S_{ch}\equiv S(\psi_{ch})=\left[1+(\alpha|\psi_{ch}|)^n\right]^{\frac{1-n}{n}}=\left[1+\left(\frac{n-1}{n}\right)^{1-2n}\right]^{\frac{1-n}{n}}. \tag{1b}$$

Here α [1/L] and n are fitting parameters of the van Genuchten model; and the saturation degree S is defined in terms of soil water content θ as $S\equiv(\theta-\theta_r)/(\theta_s-\theta_s)$, where θ_s and θ_s are the saturated and residual water contents, respectively.

The robustness and, hence, usefulness of this procedure rest on three interrelated questions. How sensitive are estimates of characteristic lengths ψ_{ae} and ψ_{ch} to a choice of the functional form of the WRC? How sensitive are these lengths to values of the WRC fitting parameters, such as α and n? Do the characteristic

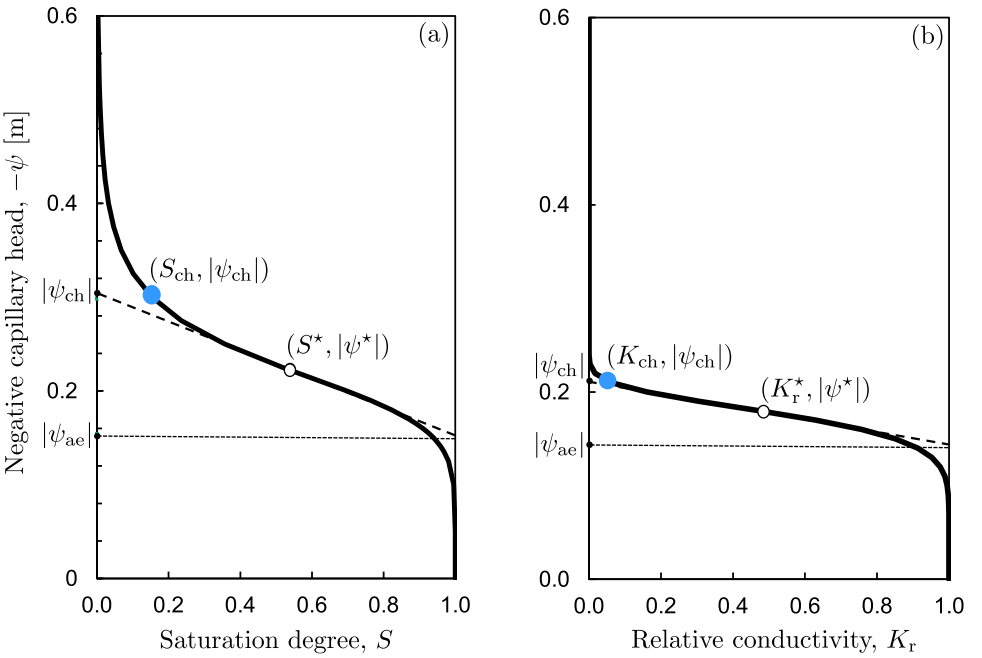

Figure 1. Linearized analysis for estimation of the characteristic lengths $|\psi_{ch}|$ and $|\psi_{ae}|$ from (a) water retention curve $S=S(\psi)$, and (b) relative hydraulic conductivity function $K_r=K_r(\psi)$. The depicted hydraulic functions correspond to the Sable de Riviere soil (Mualem, 1976).

lengths ψ_{ae} and ψ_{ch} derived from the analysis of WRC differ significantly from their counterparts derived from a similar analysis of the hydraulic conductivity function or HCF (see Figure 1b)? Our study aims to answer these questions.

We do so by considering an alternative WRC model (Assouline et al., 1998), hereinafter WRC-A,

$$S(\psi)=1-\exp\left[-\xi\left(\frac{1}{|\psi|}-\frac{1}{|\psi_L|}\right)^{\mu}\right], \qquad 0 \le |\psi| \le |\psi_L|, \tag{2}$$

where $\xi > 0$ and $\mu > 0$ are fitting parameters; and ψ_L is the capillary head corresponding to a very low water content θ_L, which represents the limit of interest for a WRC application. This model provides a physics-based link between soil structure and its hydraulic properties; its high flexibility allows for accurate representation of measured data. Parameteric equivalence between the WRC-vG and WRC-A models is established by Assouline and Or (2013). We will express characteristic lengths ψ_{ae} and ψ_{ch} in terms of fitting parameters ξ and μ of the WRC-A model, and investigate the discrepancy in the estimation of ψ_{ae} and ψ_{ch} resulting from the adoption of the two different models. This is valuable for design of evaporation experiments or estimation of available water content in a soil, which is critical for a proper irrigation design.

As mentioned above, the definition of ψ_{ch} is linked to the loss of hydraulic water continuity, which also corresponds to a drastic reduction of the unsaturated relative hydraulic conductivity $K_r(\psi)$. It is therefore reasonable to infer the values of ψ_{ae} and ψ_{ch} from HCFs rather than from WRCs (Figure 1). In this analysis, we use a HCF in the form of a Weibull distribution (Assouline & Selker, 2017),

$$K_r(\psi)=\exp\left(-\gamma|\psi|^{\omega}\right), \tag{3}$$

where γ and ω are fitting parameters. The goal here is to express ψ_{ae} and ψ_{ch} in terms of γ and ω. Finally, we investigate the sensitivity of ψ_{ae} and ψ_{ch} to values of the fitting parameters of either the WRC or the HCF. This is done by conducting a global (variance-based) sensitivity analysis (e.g., Ciriello et al., 2015; Taverniers & Tartakovsky, 2017).

This paper is arranged as follows. In section 2, we provide analytical expressions for ψ_{ae} and ψ_{ch} based on the WRC-A and HCF models. In section 3, we estimate ψ_{ae} and ψ_{ch} for a set of 15 soils, derived from the soil

catalogue of Mualem (1976). Section 4 contains a discussion of both the differences in alternative strategies for estimation of ψ_{ae} and ψ_{ch} and their practical implications. Major conclusions drawn from our study are presented in section 5.

2. Analytical Expressions for Characteristic Lengths

Analytical expressions relating ψ_{ae} and ψ_{ch} to fitting parameters ξ and μ in the WRC (2) or γ and ω in the HCF (3) are derived below.

2.1. Inference of the Characteristic Lengths From the WRC

The linearized analysis of Lehmann et al. (2008) requires one to compute a location of the inflection point of the $S=S(|\psi|)$ curve (Figure 1a). The latter satisfies an equation $\mathrm{d}^2S/\mathrm{d}|\psi|^2=0$. For the WRC in (2) this gives rise to an algebraic equation (Appendix A)

$$\frac{\xi\mu}{|\psi_L|^{\mu}}\left(\frac{1}{x}-1\right)^{\mu}+2x-(\mu+1)=0, \tag{4}$$

where $0<x\equiv|\psi|/|\psi_L|\leq 1$. Figure 1a suggests that, in the range of hydrologically relevant parameters, this equation has a unique solution which we denote by $x^\star$ or, after rescaling, $|\psi^\star|$. We show in Appendix A that

$$|\psi^\star|\approx\left(\frac{\xi\mu}{1+\mu}\right)^{1/\mu}. \tag{5}$$

The value of $S(|\psi|)$ at that point is $S^\star=S(|\psi^\star|)$.

An equation of the tangential line passing through the point $(|\psi^\star|,S^\star)$ is $S-S^\star=a(|\psi|-|\psi^\star|)$ with the slope a given by (Appendix A)

$$a=\frac{\mathrm{d}S}{\mathrm{d}|\psi|}(|\psi^\star|)=\frac{\xi\mu}{|\psi^\star|^2}\left(\frac{1}{|\psi^\star|}-\frac{1}{|\psi_L|}\right)^{\mu-1}(S^\star-1). \tag{6}$$

The definition of ψ_{ae} and ψ_{ch} in Figure 1a as points $(\psi_{ae},1)$ and $(\psi_{ch},0)$ yields analytical expressions for the characteristic lengths,

$$|\psi_{ch}|=|\psi^\star|+\frac{S^\star}{1-S^\star}\frac{|\psi^\star|^2}{\xi\mu}\left(\frac{1}{|\psi^\star|}-\frac{1}{|\psi_L|}\right)^{1-\mu},\quad |\psi_{ae}|=|\psi^\star|-\frac{|\psi^\star|^2}{\xi\mu}\left(\frac{1}{|\psi^\star|}-\frac{1}{|\psi_L|}\right)^{1-\mu}. \tag{7}$$

As before, $L_c=|\psi_{ch}|-|\psi_{ae}|$.

2.2. Inference of the Characteristic Lengths From the HCF

We show in Appendix A that the inflection point of $K_r(\psi)$ in (3) is

$$|\psi^\star|=\left(\frac{\omega-1}{\gamma\omega}\right)^{1/\omega},\qquad K_r^\star=K_r(|\psi^\star|). \tag{8}$$

An equation of the tangential line passing through the point $(|\psi^\star|,K_r^\star)$ is $K_r-K_r^\star=b(|\psi|-|\psi^\star|)$ with the slope b given by

$$b=\frac{\mathrm{d}K_r}{\mathrm{d}|\psi|}(|\psi^\star|)=-\gamma\omega\left(\frac{\omega-1}{\gamma\omega}\right)^{\frac{\omega-1}{\omega}}\exp\left(\frac{1-\omega}{\omega}\right). \tag{9}$$

The definition of ψ_{ae} and ψ_{ch} in Figure 1b as points $(\psi_{ae},1)$ and $(\psi_{ch},0)$ yields analytical expressions for the characteristic lengths,

$$|\psi_{ch}|=\left(\frac{\omega-1}{\gamma\omega}\right)^{\frac{1}{\omega}}\left(\frac{\omega}{\omega-1}\right),\qquad |\psi_{ae}|=|\psi_{ch}|+\frac{1}{b}. \tag{10}$$

Again, $L_c=|\psi_{ch}|-|\psi_{ae}|$.

Table 1
Values of γ and ω Obtained by Fitting (3), and Values of ξ and μ Obtained by Fitting (2), to the Data in Mualem (1976), *With Values of ψ and γ Expressed in Bars; Corresponding Values of ε are Computed From (11) With $\psi_L = 15$ bar*

Soil type	γ	Ω	ξ	μ	ε
Sable de Riviere	3.99×10^{14}	8.44	2.58×10^{-7}	4.48	0.23
Poudre River sand	5.20×10^{25}	17.10	2.10×10^{-9}	5.86	0.20
Rehovot sand	3.93×10^{3}	1.99	0.02	0.95	1.04
Gilat sandy loam	37.20	1.57	0.23	0.72	1.41
Rubicon sandy loam	4.33×10^{6}	5.91	5.81×10^{-5}	3.94	0.26
Pachapa fine sandy clay	2.50×10^{4}	4.20	0.12	0.92	0.95
Pachapa loam	4.58×10^{2}	2.81	0.14	1.16	0.85
Weld silty clay loam	1.44×10^{7}	5.53	1.52×10^{-5}	3.77	0.30
Amarillo silty clay loam	4.77×10^{5}	5.30	1.27×10^{-3}	2.84	0.39
Fine sand	5.33×10^{35}	24.20	3.27×10^{-7}	4.44	0.25
Touchet silt loam	1.02×10^{6}	5.00	3.71×10^{-5}	3.86	0.29
Sand	1.58×10^{7}	5.35	2.20×10^{-4}	2.82	0.38
Sinai sand	7.13×10^{7}	5.41	1.38×10^{-4}	2.78	0.39
Adelaide dune sand	2.29×10^{6}	5.08	1.05×10^{-3}	2.63	0.41
Bet Dagan sandy loam	6.94×10^{4}	3.14	9.03×10^{-3}	1.44	0.71

3. Application to Field Data

We use a data set of 15 soils, including experimental data relevant to the definition of the appropriate hydraulic functions (WRC and HCF), compiled from the soil catalogue of Mualem (1976). This data set includes a wide variety of soil types, ranging from sand to silty clay loam. Values of the fitting parameters in WRC (2) and HCF (3) for these soils are reported in Table 1, together with corresponding values of the parameter ε,

$$\varepsilon = \frac{1}{\Gamma(1+1/\mu)+1/|\psi_L|}\sqrt{\Gamma(1+2/\mu)-\Gamma(1+1/\mu)^2}, \qquad (11)$$

which characterizes the WRC-A through its coefficient of variation (Assouline, 2001, 2005; Assouline et al., 1998). In (11), $\Gamma(\cdot)$ denotes the complete gamma function.

Estimated values of ψ_{ae} and ψ_{ch} are alternatively computed using (7) for WRC (2) or using (10) for HCF (3). These values are compared to estimates resulting from the application of (1) for the van Genuchten WRC. For each ψ_{ch}, corresponding values of S and K_r are computed based on the selected WRC model and related HCF expressions, as derived from the Mualem formulation (Assouline & Or, 2013; Assouline & Tartakovsky, 2001).

A variance-based global sensitivity analysis (GSA) is used to ascertain the influence of parametric uncertainty on the estimates of ψ_{ae}, ψ_{ch}, and $L_c = |\psi_{ch}| - |\psi_{ae}|$ obtained with the WRC-A or HCF models. We treat ξ and μ in WRC-A (2) and γ and ω in HCF (3) as random variables uniformly distributed within the range of values collected in Table 1. For the WRC-A model, the values of the first-order Sobol' indices for ξ and μ are $\mathcal{S}_\xi = 0.141$ and $\mathcal{S}_\mu = 0.846$ in the case of ψ_{ae}, and $\mathcal{S}_\xi = 0.413$ and $\mathcal{S}_\mu = 0.570$ in the case of ψ_{ch}. This means that uncertainty in ξ contributes less to uncertainty in estimates of ψ_{ae} than uncertainty in μ does; uncertainty in ξ and μ have roughly the same impact on estimates of ψ_{ch}. The Sobol' indices for L_c are $\mathcal{S}_\xi = 0.599$ and $\mathcal{S}_\mu = 0.252$, indicating the importance of uncertainty in both parameters.

When characteristic lengths ψ_{ae} and ψ_{ch} are estimated from the HCF model, the values of the first-order Sobol' indices for γ and ω are $\mathcal{S}_\gamma =$

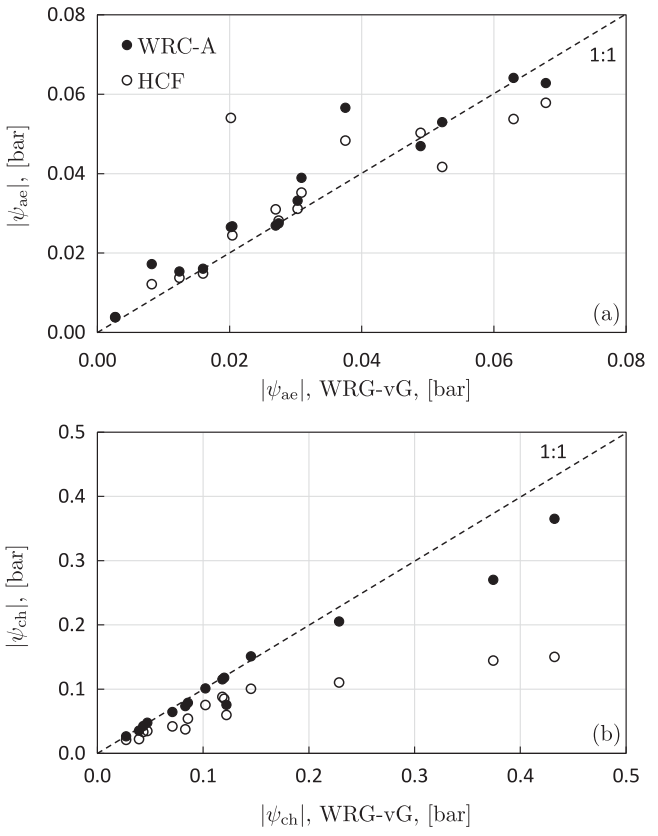

Figure 2. Estimates of (a) air-entry head ψ_{ae} and (b) critical capillary head ψ_{ch}, for soils included in the data set of (Mualem, 1976, Table 1), based on the WRC-A model (black dots) and the HCF model (white dots), both compared to estimates inferred from the WRC-vG model.

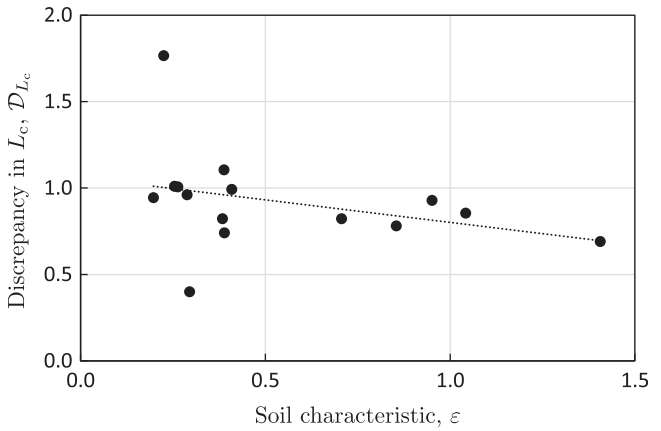

Figure 3. Dependence on soil characteristic ε of the discrepancy in estimates of L_c (or ψ_{ch}) inferred from the WRC-A and WRC-vG models, $\mathcal{D}_{L_c}=L_{c,WRC-A}/L_{c,WRC-vG}$.

0.00137 and $\mathcal{S}_\omega=0.997$ in the case of ψ_{ae}, and $\mathcal{S}_\gamma=0.00142$ and $\mathcal{S}_\omega=0.997$ in the case of ψ_{ch}. This indicates that uncertainty in ω dominates uncertainty in estimates of both ψ_{ae} and ψ_{ch}, i.e., extra care should be paid to experimental determination of ω. The Sobol' indices for L_c are $\mathcal{S}_\gamma=0.00186$ and $\mathcal{S}_\omega=0.996$, thus confirming the predominant role of ω as a source of uncertainty. These GSA results are obtained by applying a polynomial chaos expansion technique (see Ciriello et al., 2015 for more detail).

4. Discussion

Figure 2 compares estimates of ψ_{ae} and ψ_{ch} obtained from either WRC-A or HCF with those inferred from the WRC-vG model. The values of ψ_{ae} are not significantly affected by the model chosen to represent the WRC or by considering the HCF instead (Figure 2a). This suggests that departure from the saturated water content θ_s occurs almost at the same capillary head as departure from the saturated hydraulic conductivity K_s. This is an interesting result since ψ_{ae} is found to be a robust characteristic length, allowing predictions of the hydraulic conductivity of a wide range of natural and compacted earth materials, from rocks to soils (Assouline & Or, 2008).

On the contrary, the model selection becomes more relevant for determination of ψ_{ch} (Figure 2b). When the WRC-A model is applied, the values are similar for $\psi_{ch} < 0.15$ bar, which corresponds to sandy soils, while significant differences are observed for the range of clayey soils. The HCF-based approach significantly underestimates ψ_{ch} for the whole range of soil types. As an example, the WRC-vG model predicts $\psi_{ch}=0.43$ bar, while the WRC-A and HCF models yield $\psi_{ch}=0.37$ bar and 0.15 bar, respectively.

When evaporation is considered, it is preferable to estimate ψ_{ch} from a WRC, since the latter is related to the continuity of capillary pathways to the soil surface. Discrepancy in estimation of L_c (or ψ_{ch}) with either the WRC-A or the WRC-vG, $\mathcal{D}_{L_c}=L_{c,WRC-A}/L_{c,WRC-vG}$, is shown in Figure 3 as a function of soil characteristic ε. For soils with low ε (say, $\varepsilon < 0.3$), the discrepancy is small, i.e., the impact of model selection is relatively minor. For soils with higher ε, and especially for $\varepsilon > 0.5$, the values of L_c estimated with the WRC-vG are 20% higher than those inferred from the WRC-A. A value of L_c is critical to the design of evaporation experiments in columns, as it determines a minimal column length for which transition from capillary-supplied (stage I) to vapor diffusion-controlled (stage II) evaporation is governed by soil hydraulic property rather than by the column's length. Therefore, one might want to fit several WRC models to experimental data and use a largest estimate of L_c to determine the length of an evaporative column.

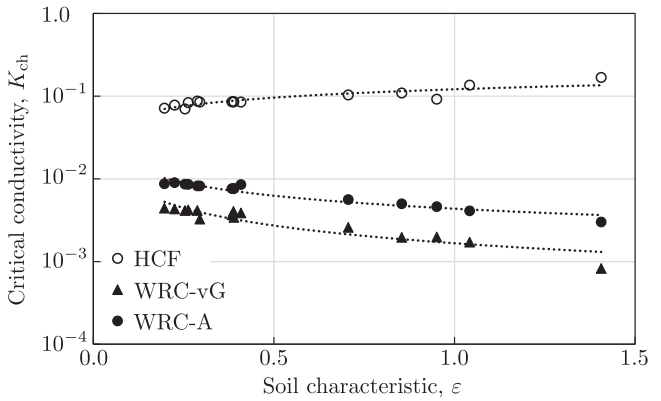

Figure 4. Dependence on soil characteristic ε of critical relative hydraulic conductivity, $K_{ch} \equiv K_r(\psi_{ch})$, wherein values of ψ_{ch} are alternatively inferred from the WRC-A, WRC-vG, or HCF models.

If ψ_{ch} has been estimated from a WRC, then a corresponding value of the relative hydraulic conductivity, $K_{ch}=K_r(\psi_{ch})$, can be computed from a model linking the WRC to a HCF (Assouline & Or, 2013; Assouline & Tartakovsky, 2001). If, on the other hand, ψ_{ch} has been estimated from a HCF, then computing $K_{ch}=K_r(\psi_{ch})$ is straightforward. Values of K_{ch} computed with these alternative approaches are shown in Figure 4 as a function of ε. The discrepancy in estimators of ψ_{ch} from alternative models is amplified when computing K_{ch}; that is because K_{ch} depends nonlinearly on ψ_{ch}, while L_c is directly proportional to ψ_{ch}. The HCF approach predicts an order-of-magnitude drop in unsaturated hydraulic conductivity at capillary head values (ψ_{ch}), i.e., $K_{ch} \sim 0.1$ or $K(\psi) \sim 0.1K_s$; the WRC-based approaches predict between 2 and 3 orders of magnitude reduction in conductivity. The WRC-vG approach leads to lowest estimates of K_{ch}, with estimates of K_{ch} inferred from the WRC-A being approximately twice as large as those from the WRC-vG. Estimates of K_{ch} from the WRCs decrease with ε, while their counterparts obtained from the the HCF increases.

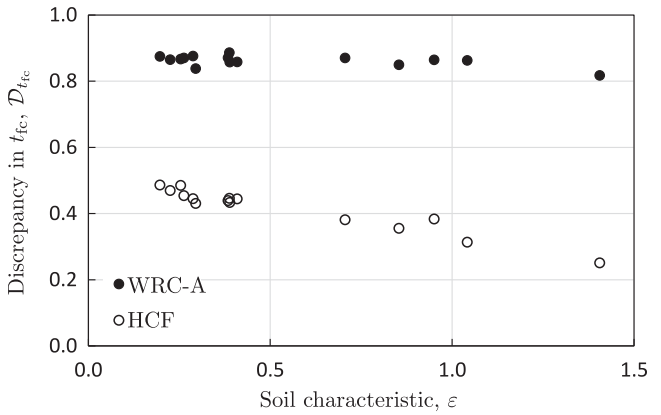

Figure 5. Dependence on ε of the time required to attain filed capacity, t_{fc}, corresponding to the $K_{ch}=K_r(\psi_{ch})$ estimated from the WRC-A (black dots) or HCF (white dots) models, relative to the t_{fc} inferred from the WRC-vG model.

Physical considerations suggest that the HCF approach should be used to estimate K_{ch} when modeling drainage and/or characterizing field capacity. Specifically, K_{ch} is directly linked to the time required to attain filed capacity, t_{fc} (Assouline & Or, 2014). For a draining soil, the latter is given by an analytical solution of Youngs (1960),

$$t_{fc}=-\frac{Q_\infty}{K_s}\ln\left[K_r(S_{ch})\right], \tag{12}$$

where $Q_\infty=z[\theta(z)-\theta_r]$ is the total drainable water (equivalent water depth) at soil depth z after "infinite" time. Taking the WRC-vG approach as a basis, we define the discrepancy $\mathcal{D}_{t_{fc}}$ between its estimate of t_{fc} and those inferred from either the WRC-A or the HCF as

$$\mathcal{D}_{t_{fc}}=\frac{t_{fc,i}}{t_{fc-vG}}=\frac{\{\ln\left[K_r(\psi_{ch})\right]\}_i}{\ln\left[K_{r-vG}(\psi_{ch})\right]}, \qquad i=\text{WRC}-\text{A or HCF}. \tag{13}$$

Figure 5 reveals that reliance on the WRC-A reduces estimates of t_{fc} by 10% to 15%. The HCF approach leads to a more significant discrepancy, which becomes more pronounced as ε increases: for $\varepsilon\sim0.2$, the HCF-based estimate of t_{fc} is about half of that based on the WRC-vG, while for $\varepsilon\sim1.5$, this ratio reduces to 1/5. This finding demonstrates that expressing t_{fc} in terms of a drop in hydraulic conductivity, rather than in terms of a loss of capillary pathways, predicts a much faster attainment of field capacity.

Field capacity can also be characterized by a critical saturation degree S_{ch}, which we relate to the corresponding values of ψ_{ch} estimated with the three alternative approaches. Figure 6 exhibits these alternative estimates of S_{ch}, plotted as a function of ε. Both WRC-based approaches predict an approximately linear increase of S_{ch} with ε; the WRC-A returns values higher (about 20% on average) than the WRC-vG. This linear trend vanishes when the HCF approach is applied, in which case estimates of S_{ch} are appreciably higher and independent of ε ($S_{ch}\approx0.6\pm0.1$).

This finding has significant implications for irrigation design, since irrigation demand is partially determined by soil available water capacity (Veihmeyer & Hendrickson, 1927),

$$\text{AWC}=\theta_{ch}-\theta_{wp}, \tag{14}$$

where θ_{wp} is a water content at the plant wilting point. The latter is often assumed to correspond to the residual water content, θ_r, at tension of $-\psi=15$ bars. As a result, AWC, normalized with the total water content $\theta_s-\theta_r$, is similar to S_{ch}. For soils characterized by $\varepsilon>1.0$, the relative AWC is not significantly affected by the approach used for its estimation. However, for soils characterized by low ε, and especially those with $\varepsilon<0.5$, which generally corresponds to sandy soils, large differences in the relative AWC may lead to strong constraints on irrigation amount and frequency (lower AWC requiring smaller irrigation doses, applied more frequently).

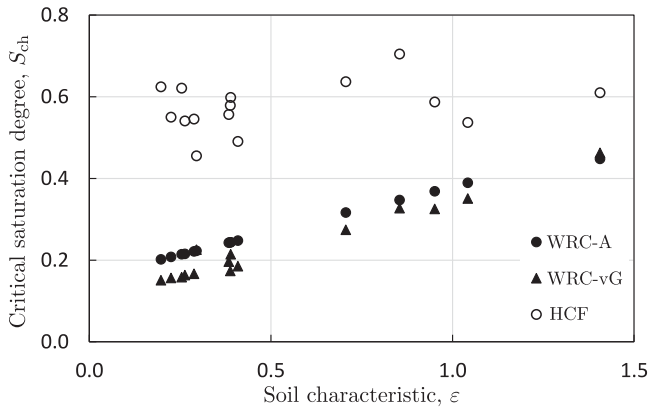

Figure 6. Dependence on ε of the saturation degree S_{ch} estimated from the WRC-A (black dots), WRC-vG (black triangles), or HCF (white dots) models.

5. Conclusions

Characteristic length scales of flow in partially saturated porous media are related to two concurrent physical conditions: the existence of a capillary gradient that drives the flow, and the presence of continuous capillary pathways. Our analysis of soil water retention curves reveals that these conditions are simultaneously fulfilled only within the range of drainable soil pores, between the air-entry value, ψ_{ae}, and the critical capillary head, ψ_{ch}. These parameters are computed analytically as inflection points of either a water retention curve (WRC) or a hydraulic conductivity function (HCF). Consequently, their values are affected by the choice of a functional form of these constitutive relations. Our study had two major goals: to determine the impact of model selection on estimates of ψ_{ae} and

ψ_{ch}, and to quantify the sensitivity of these estimates to (possibly uncertain) soil parameters. Our analysis leads to the following major conclusions.

1. The value of ψ_{ae} is not significantly affected either by the WRC model selection or by the reliance on the HCF instead. This parameter serves as a robust characteristic length allowing one to predict hydraulic conductivity of a wide range of natural or compacted earth materials, from rocks to soils (Assouline & Or, 2008).
2. The WRC model selection has only marginal impact on the value of ψ_{ch} for sandy soils; this impact becomes significant for clayey soils.
3. The value of $L_c=|\psi_{ch}|-|\psi_{ae}|$ is critical for the design of evaporation column experiments, as it determines the minimum column length that assures that transition from the capillary-supplied stage of evaporation to the vapor diffusion-controlled stage is governed by soil hydraulic properties rather than by an arbitrary column length. Hence, ψ_{ch} should be inferred from a WRC model when the evaporation process is considered.
4. Determination of ψ_{ch} from a HCF yields significantly higher estimates (lower absolute values) relative to those resulting from the corresponding WRC, for the whole range of soil types.
5. Linking the attainment of field capacity to a drop in hydraulic conductivity rather than to a loss of capillary pathways simulates a much faster attainment of field capacity.
6. Differences in estimates of the available water content for plants, for sandy soils could stem from the evaluation of ψ_{ch} based on the WRC or the HCF.

Appendix A: Derivation of Analytical Expressions for Characteristic Lengths

It follows from (2) that

$$\frac{\mathrm{d}^2S}{\mathrm{d}|\psi|^2}=\frac{\xi^2\mu^2}{|\psi|^4}\left[\left(\frac{1}{|\psi|}-\frac{1}{|\psi_L|}\right)^{2\mu-2}+\frac{2|\psi|-|\psi_L|(1+\mu)}{\xi\mu|\psi_L|}\left(\frac{1}{|\psi|}-\frac{1}{|\psi_L|}\right)^{\mu-2}\right](S-1). \tag{A1}$$

Setting this to 0 yields (4). Rewriting (4) as

$$\epsilon\left(\frac{1}{x}-1\right)^{\mu}+2x-(\mu+1)=0,\qquad \epsilon\equiv\frac{\xi\mu}{|\psi_L|^{\mu}}\ll 1 \tag{A2}$$

with $0<x\leq 1$ suggests a leading-order (in ϵ) solution $x^*=(1+\mu)/2$, which is not valid for $\mu>1$. Instead we recast it as

$$\epsilon(1-x)^{\mu}+2x^{1+\mu}-(1+\mu)x^{\mu}=0, \tag{A3}$$

and expand the first term into a binomial series to obtain

$$\epsilon\sum_{n=0}^{\infty}(-1)^n\binom{\mu}{n}x^n+2x^{1+\mu}-(1+\mu)x^{\mu}=0,\qquad \binom{\mu}{n}=\frac{\mu(\mu-1)\ldots(\mu-n+1)}{n!}. \tag{A4}$$

Neglecting the higher-order terms, this yields $\epsilon(1-x)+2x^{1+\mu}-(1+\mu)x^{\mu}=0$. Equating the leading-order terms,

$$\epsilon-(1+\mu)x^{\mu}=0\qquad\Rightarrow\qquad x=\left(\frac{\epsilon}{1+\mu}\right)^{1/\mu}. \tag{A5}$$

Recalling the definitions of ϵ and x, we arrive at (5).

It follows from (3) that

$$\frac{\mathrm{d}^2K_r}{\mathrm{d}|\psi|^2}=\gamma\omega\exp\left(-\gamma|\psi|^{\omega}\right)|\psi|^{\omega-2}[\gamma\omega|\psi|^{\omega}+1-\omega]. \tag{A6}$$

Setting this to 0 yields (8).

Acknowledgments
The data used are listed in the references and tables. This work was supported in part by the National Science Foundation under grant NSF-CBET-1563614.

References

Assouline, S. (2001). A model of soil relative hydraulic conductivity based on water retention curve characteristics. *Water Resources Research*, *37*, 265–271.
Assouline, S. (2005). On the relationship between the pore size distribution index and characteristics of the soil hydraulic functions. *Water Resources Research*, *41*, W07019. https://doi.org/10.1029/2004WR003511
Assouline, S., & Or, D. (2008). Air entry-based characteristic length for estimation of permeability of variably compacted earth materials. *Water Resources Research*, *44*, W11403. https://doi.org/10.1029/2008WR006937
Assouline, S., & Or, D. (2013). Conceptual and parametric representation of soil hydraulic properties: A review. *Vadose Zone Journal*, *12*, 1–20. https://doi.org/10.2136/vzj2013.07.0121
Assouline, S., & Or, D. (2014). The concept of field capacity revisited: Defining intrinsic static and dynamic criteria for soil internal drainage dynamics. *Water Resources Research*, *50*, 4787–4802. https://doi.org/10.1002/2014WR015475
Assouline, S., & Selker, J. S. (2017). Introduction and evaluation of a Weibull hydraulic conductivity-pressure head relationship for unsaturated soils. *Water Resources Research*, *53*, 4956–4964. https://doi.org/10.1002/2017WR020796
Assouline, S., & Tartakovsky, D. M. (2001). Unsaturated hydraulic conductivity function based on a soil fragmentation process. *Water Resources Research*, *37*, 1309–1312.
Assouline, S., Tessier, D., & Bruand, A. (1998). A conceptual model of the soil water retention curve. *Water Resources Research*, *34*, 223–231.
Ciriello, V., Edery, Y., Guadagnini, A., & Berkowitz, B. (2015). Multimodel framework for characterization of transport in porous media. *Water Resources Research*, *51*, 3384–3402. https://doi.org/10.1002/2015WR017047
Hoogland, F., Lehmann, P., & Or, D. (2016). Drainage dynamics controlled by corner flow: Application of the foam drainage equation. *Water Resources Research*, *52*, 8402–8412. https://doi.org/10.1002/2016WR019299
Lehmann, P., Assouline, S., & Or, D. (2008). Characteristics lengths affecting evaporative drying from porous media. *Physics Review. E*, *77*, 056309. https://doi.org/10.1103/PhysRevE.77.056309
Miller, E. E., & Miller, R. D. (1956). Physical theory for capillary flow phenomena. *Journal of Applied Physics*, *27*, 324–332.
Mualem, Y. (1976). *A catalogue of the hydraulic properties of unsaturated soils, Technion* (Research Project 442, 100 pp.). Haifa, Israel: Israel Institute of Technology.
Or, D., Lehmann, P., & Assouline, S. (2015). Natural lengths scales define the range of applicability of the Richards equation for capillary flows. *Water Resources Research*, *51*, 7130–7144. https://doi.org/10.1002/2015WR017034
Or, D., Lehmann, P., Shahraeeni, E., & Shokri, N. (2013). Advances in soil evaporation: A review. *Vadose Zone Journal*, *12*(4). https://doi.org/10.2136/vzj2012.0163
Roth, K. (2008). Scaling of water flow through porous media and soils. *European Journal Soil Science*, *59*, 125–130.
Sposito, G., & Jury, W. A. (1985). Inspectional analysis in the theory of water flow through unsaturated soil. *Soil Science Society of America Journal*, *49*, 791–798.
Taverniers, S., & Tartakovsky, D. M. (2017). Impact of parametric uncertainty on estimation of the energy deposition into an irradiated brain tumor. *Journal of Computational Physics*, *348*, 139–150. https://doi.org/10.1016/j.jcp.2017.07.008
Tillotson, P. M., & Nielsen, D. R. (1984). Scale factors in soil science. *Soil Science Society of America Journal*, *48*, 953–959.
Veihmeyer, F. J., & Hendrickson, A. H. (1927). The relation of soil moisture to cultivation and plant growth. *Proceedings of First International Congress of Soil Science*, *3*, 498–513.
Youngs, E. G. (1960). The drainage of liquids from porous materials. *Journal of Geophysical Research*, *65*, 4025–4030.